

Inequality constraints in variational quantum circuits with qudits

Alberto Bottarelli,^{1,2} Sebastian Schmitt,³ and Philipp Hauke^{1,2}

¹*Pitaevskii BEC Center, CNR-INO and Dipartimento di Fisica, Università di Trento, I-38123 Trento, Italy*

²*INFN-TIFPA, Trento Institute for Fundamental Physics and Applications, Trento, Italy*

³*Honda Research Institute Europe GmbH, Carl-Legien-Str. 30, 63073 Offenbach, Germany*

(Dated: October 11, 2024)

Quantum optimization is emerging as a prominent candidate for exploiting the capabilities of near-term quantum devices. Many application-relevant optimization tasks require the inclusion of inequality constraints, usually handled by enlarging the Hilbert space through the addition of slack variables. This approach, however, requires significant additional resources especially when considering multiple constraints. Here, we study an alternative direct implementation of these constraints within the QAOA algorithm, achieved using qudit-SUM gates, and compare it to the slack variable method generalized to qudits. We benchmark these approaches on three paradigmatic optimization problems. We find that the direct implementation of the inequality penalties vastly outperforms the slack variables method, especially when studying real-world inspired problems with many constraints. Within the direct penalty implementation, a linear energy penalty for unfeasible states outperforms other investigated functional forms, such as the canonical quadratic penalty. The proposed approach may thus be an enabling step for approaching realistic industry-scale and fundamental science problems with large numbers of inequality constraints.

I. INTRODUCTION

In recent years, quantum optimization [1, 2] has emerged as a highly promising field within near term quantum computation, as it may help to solve combinatorial optimization problems prevalent in both physics and industrial applications. Examples include Max-Cut, k -sat, various portfolio management, scheduling, and assignment problems. Numerous quantum algorithms have been developed to tackle these optimization tasks, leveraging different concepts such as adiabaticity, employed in quantum annealing [3, 4], or the variational principle, at the basis of the Variational Quantum Eigensolver (VQE) [5–8] or Quantum Approximate Optimization Algorithm (QAOA) [9, 10]. These algorithms have in common that they formulate the optimization problem in terms of a cost function $C(\mathbf{x})$ defined on the boolean cube, where the objective is to find a string $\mathbf{x} \in \{0, 1\}^N$ that minimizes or maximizes $C(\mathbf{x})$. For realistic applications, a central aspect is given by the presence of (typically many) constraints. See, for example, Ref. [11] for a recent example from the electromobility domain. These are commonly implemented in quantum optimization routines by adding a penalty function in the cost Hamiltonian, analogous to classical optimization approaches. However, often the constraints are of inequality type, whose realization, typically done in the form of slack variables, requires significant overhead compared to equality constraints. The inclusion of inequality constraints thus represents a major bottleneck for realistic quantum-optimization protocols, in particular for their implementations on current noisy intermediate-scale quantum (NISQ) hardware.

Here, we propose an approach based on the direct implementation of the inequality-constraint energy penalty as diagonal unitaries using qudit SUM-gates. We discuss the necessary resource scaling in terms of qudit levels and gates and compare it to the standard constraint-

handling approach based on slack variables. We show that for a specific class of constraints, we obtain an exponential reduction in the number of gates needed to implement the energy penalty. We illustrate the direct energy penalty on three different problems, a randomly interacting Ising spin model, a constrained state sampling problem, and an electric vehicle (EV) charging problem [see Fig. 1(a,b)], and benchmark it against the slack-variable approach using exact numerical simulations of a QAOA protocol [Fig. 1(c)]. As a further advantage, the functional form of the direct energy penalty can be chosen essentially at will. Generically, we find the precise form of the energy penalty [Fig. 1(d)] to have a significant influence on the performance of the quantum optimization protocol. In particular, a linear function outperforms other forms, such as a constant or a quadratic function. Furthermore, we find that the proposed direct unitary method performs better than the slack variable state-of-the-art method, especially when multiple constraints have to be considered.

This enhancement is facilitated by tapping into the rapid recent developments in qudit quantum information processing. Precise and universal control of quantum systems with $d > 2$ levels has been realized on various platforms ranging from trapped ions, over neutral atoms, to superconducting systems [12–19]. By compressing quantum information into higher-dimensional objects, the use of qudits is particularly appealing in the NISQ-era, where even a constant or polynomial saving of resources can have a significant effect. The usefulness of qudits has been discussed for example in the context of combinatorial quantum optimization problems [20–23], where the natural description is in terms of d -ary integer variables $x_i \in \{0, \dots, d-1\}$ rather than only binary variables. Our results illustrate another useful application by using ancilla qudits to implement inequality constraints as a direct energy penalty in the cost function may generate a significant performance advantage

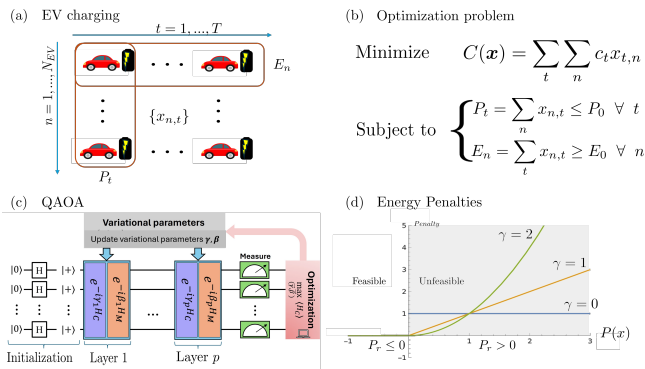


FIG. 1. Schematic representation of the aspects of an electric vehicle (EV) charging problem as a typical realistic optimization problem. (a) Sketch of the problem structure where N_{EV} EVs need to be charged over a period of T time steps. (b) The cost function to minimize and the constraints, which represent maximal charging power at each time step (indicated by the vertical red squares in panel (a)) and minimum charged energy required for each EV (horizontal red squares in (a)). (c) Form of the proposed energy penalty terms that distinguish feasible and unfeasible configurations and thus allow to enforce inequality constraints. (d) Schematic representation of the QAOA procedure..

for realistic optimization problems.

The remainder of this paper is organized as follows. In Sec. II, we recap QAOA for qubit and qudit systems. In Sec. III, we discuss possible ways of imposing constraints on the solutions of the problem. In particular, we compare their resource scaling for the standard approach via slack variables and the method that is the main subject of this study, the inclusion of a nonlinear energy penalty in the cost function. Section IV presents a numerical study of the approaches described in previous sections, showing the beneficial performance of the direct approach to constraints through diagonal unitaries. We present our conclusions in Sec. V. Technical details and explicit circuits used in order to introduce the penalties are reported in the Appendix.

II. REVIEW OF THE QUANTUM APPROXIMATE OPTIMIZATION ALGORITHM (QAOA)

The quantum approximate optimization algorithm (QAOA) [9, 10, 24] is a hybrid variational quantum algorithm [1, 5] designed to solve combinatorial optimization problems. Its schematic is shown in Fig. 1 (c). Given a cost function $C(\mathbf{x})$ of N classical variables $\mathbf{x} = (x_1, \dots, x_N)$, QAOA aims at finding the solution to

$$\min_{\mathbf{x} \in \{0,1\}^N} C(\mathbf{x}), \quad (1)$$

yielding the corresponding optimal configuration \mathbf{x}_{\min} . For now, we assume as usual the variables to be binary, $x_i \in \{0, 1\}$. Extending this scheme to multi-level qudits

is straight-forward and is described below. An important class of problems that is usually addressed with QAOA consists of quadratic unconstrained binary optimization (QUBO) problems [25] whose cost function is expressed as

$$C(\mathbf{x}) = 4\mathbf{x}^T J \mathbf{x} = 4 \sum_{i,j=1}^N J_{ij} x_i x_j, \quad (2)$$

where J is a symmetric and real $N \times N$ cost matrix, and where we included a factor of 4 for convenience. Such QUBO problems are important for industrial applications, as many paradigmatic problems can be mapped onto such a form [4, 26], as well as for physics questions given their equivalence to Ising Hamiltonians.

In order to solve the problem using quantum computation, one promotes the classical variables to operators acting on a Hilbert space $\mathcal{H}_C = \mathbb{C}^{2^N}$. This is usually defined as

$$x_i \rightarrow \frac{1 + \sigma_z^i}{2}, \quad (3)$$

where σ_z^i is the z -Pauli spin operator for qubit i . The cost function $C(\mathbf{x})$ is promoted to a Hamiltonian H_C by replacing each variable with the corresponding operator, as indicated in Eq. (3). Each state of the computational basis $\{|\mathbf{x}\rangle\}$ represents a classical bit string \mathbf{x} and H_C is diagonal on this basis with eigenvalues $C(\mathbf{x})$:

$$H_C |\mathbf{x}\rangle = C(\mathbf{x}) |\mathbf{x}\rangle. \quad (4)$$

The solution of the optimization problem is thus encoded in the ground state of the Ising Hamiltonian

$$H_C = \sum_{i,j} J_{ij} \sigma_i^z \sigma_j^z + \sum_i h_i \sigma_i^z. \quad (5)$$

The QAOA ansatz for finding the ground state of H_C consists in preparing a parametrized trial state

$$|\psi(\boldsymbol{\alpha}, \boldsymbol{\beta})\rangle = U(\boldsymbol{\alpha}, \boldsymbol{\beta}) |\psi_0\rangle, \quad (6)$$

generated by alternating parametrized unitaries in the following way:

$$U(\boldsymbol{\alpha}, \boldsymbol{\beta}) = \prod_{l=1}^p e^{i\alpha_l H_C} e^{i\beta_l H_M}. \quad (7)$$

In the above, $|\psi_0\rangle$ is usually taken to be $\frac{1}{\sqrt{D}} \sum_{\mathbf{x}} |\mathbf{x}\rangle$, with $D = \dim \mathcal{H}_C = 2^N$ the Hilbert space dimension and $|\mathbf{x}\rangle$ all the possible states of the computational basis. A schematic representation of this circuit is shown in Fig. 1(c). Apart from a diagonal cost Hamiltonian H_C , the state is acted on with a non-diagonal mixing operator H_M , which has the role of inducing transitions between the different states. It is thus fundamental that the mixing operator and the cost Hamiltonian do not commute, i.e., $[H_C, H_M] \neq 0$. Due to the formulation of cost Hamiltonians in terms of Pauli σ_z operators, the

most common mixer has the form $H_M = \sum_i \sigma_i^x$, which is also used in this work. The depth of the ansatz is defined by the integer hyperparameter p , also known as the number of layers of the algorithm. The expectation value of the cost Hamiltonian is calculated with the trial state of Eq. (6) as

$$E(\boldsymbol{\alpha}, \boldsymbol{\beta}) = \langle \psi(\boldsymbol{\alpha}, \boldsymbol{\beta}) | H_C | \psi(\boldsymbol{\alpha}, \boldsymbol{\beta}) \rangle. \quad (8)$$

The set of $2p$ variational parameters $(\boldsymbol{\alpha}, \boldsymbol{\beta})$ is used to minimize the expectation value by a classical optimization routine. Due to the variational principle, this value is ensured to be an upper bound to the ground state energy of H_C .

It is rather straightforward to generalize QAOA to solve problems formulated with d -ary integer variables $x_i \in \{0, \dots, d-1\}$ which are represented by qudits. The local Hilbert space dimension of each operator representing classical variables becomes \mathbb{C}^d and the Pauli matrices are replaced with angular momentum operators $\{L_x, L_y, L_z\}$ with representation index $\ell = \frac{d-1}{2}$. Given a cost function $C(\mathbf{x})$ defined in terms of such d -ary variables, the quantum-mechanical cost Hamiltonian is obtained by replacing each variable as

$$x_i \rightarrow L_z^i + \frac{d-1}{2}. \quad (9)$$

For qudits, the available unitaries are given by the operators of the group $SU(d)$, which has $d^2 - 1$ generators. To be able to generate all possible unitaries, it is necessary to modify the mixing operator. To the trivial generalization $H_M = \sum_{i=1}^N L_x^i$, we add a squeezing operator $\sum_i (L_z^i)^2$. It was shown [14, 27] that the set $\{L_z^i, (L_z^i)^2, L_x^i\}$ allows to generate all possible unitaries of $SU(d)$ by repeated finite rotations of the qudit. Therefore, we use the mixer for qudits in the form

$$H_M = \sum_i (\beta L_x^i + \gamma (L_z^i)^2). \quad (10)$$

Once the cost Hamiltonian and the mixer are defined, the algorithm works in the same way as the qubit version. Below, we will use qudits only for implementing the slack variables, though many application-relevant cost functions can naturally benefit from formulation in terms of qudits [20–22, 28–32].

III. CONSTRAINT HANDLING IN QAOA

For many physical and industrial problems, minimizing a cost function as in Eq. (1) does not necessarily suffice to give the desired solution. Often, the problem is subject to a set of additional constraints that need to be fulfilled. Constraints that are expressed as equalities are usually handled in the context of quantum optimization by adding quadratic energy penalties to the problem Hamiltonian, such that unfeasible states are shifted to higher energy [4, 33]. In contrast, inequality constraints are generally harder to include and lead

to less efficient encodings. These are the subject of this work.

We focus on optimization problems of the form

$$\mathbf{x}_{\min} = \operatorname{argmin}_{\mathbf{x} \in \{0,1\}^N} C(\mathbf{x}) \quad (11)$$

subject to R inequality constraints

$$P_r(\mathbf{x}) \leq 0, \quad r = \{1, \dots, R\}, \quad (12)$$

where r labels all the constraints included in the problem and $P_r(\mathbf{x})$ is a classical function of the search variables characterizing the constraint.

The current state of the art for incorporating inequality constraints into quantum algorithms consists in converting inequalities into equalities by the use of slack variables and adding corresponding quadratic penalty terms to the Hamiltonian [4]. In contrast to purely qubit based methods, we will employ qudit slack variables, which avoid the overhead of encoding larger integers into multi binary variables and thus can be seen as a best-case scenario for slack variable approaches (Sec. III A). In addition, we propose a novel direct implementation of energy-penalties, which acts only on the unfeasible subspace (Sec. III B) and allows to keep the structure of the variational algorithm unchanged (schematics in Fig. 1 (c)). In our numerical benchmarks in the next section, we compare this proposed approach to the qudit-based slack-variable implementation. For completeness, other possible approaches for inequality-constraint handling that have been discussed in the literature are mentioned in Sec. III C.

A. Slack variables as qudit operators

The standard approach to introduce inequality constraints in QAOA is via the use of slack variables [4]. Here, we first give a short review of slack variables for classical optimization problems and then discuss how to use qudits in order to encode them in quantum optimization algorithms. We assume the function $P_r(\mathbf{x})$ to have N_r possible values, i.e., $P_r(\mathbf{x}) \in \{p_1, \dots, p_{N_r}\} \forall \mathbf{x}$. Of these values, the first N_r^{feas} are negative or zero (i.e., they denote feasible solutions) and $N_r - N_r^{\text{feas}}$ are greater than zero (i.e., they denote unfeasible solutions). The inequality constraint can be transformed into equality constraints with the introduction of an appropriate slack variable s_r such that

$$P_r(\mathbf{x}) \leq 0 \quad (13)$$

$$\Leftrightarrow P_r(\mathbf{x}) + s_r = 0. \quad (14)$$

The slack variables take non-negative values ($s_r \geq 0$) and their range is determined by the values the constraint function attains for feasible configurations such that only when Eq. (13) is satisfied a value for s_r can be found such that Eq. (14) is satisfied. Technically, $s_r \in \{-P_r(\mathbf{x}) : \forall \text{ feasible } \mathbf{x}\}$.

The penalized cost function considering all R different constraints can then be expressed as:

$$C_{\text{slack}}(\mathbf{x}) = C(\mathbf{x}) + \sum_{r=1}^R \lambda_r (P_r(\mathbf{x}) + s_r)^2, \quad (15)$$

where one slack variable s_r needs to be introduced for each inequality constraint, and each term gets a penalty factor $\lambda_r > 0$. If the slack variables are encoded into binary degrees of freedom, as is usually done, one requires at least $\sum_r \log_2 N_r^{\text{feas}}$ auxiliary binary variables for a given constraint s_r with N_r^{feas} allowed values [34]. Typically, N_r is larger than 2, rendering the associated spatial resource overhead rather costly, especially for current NISQ devices.

This resource overhead can be reduced by the use of qudits to represent the slack variables. If the qudit dimension d matches the number of feasible values N_r , the computational basis needs to be extended by one qudit state for each constraint, i.e., slack variable,

$$|\mathbf{x}\rangle \Rightarrow |\mathbf{x}, \{s_1, \dots, s_R\}\rangle \equiv |\mathbf{x}, \mathbf{s}\rangle. \quad (16)$$

In the quantum formulation, the constraint function as well as the slack variable are represented by operators with the appropriate eigenvalues,

$$(\hat{P}_r + \hat{S}_r) |\mathbf{x}, \mathbf{s}\rangle = (P_r(\mathbf{x}) + s_r) |\mathbf{x}, \mathbf{s}\rangle. \quad (17)$$

With this formulation, feasible configurations of the search variables \mathbf{x} can be identified by finding the appropriate basis state where the qudit slack variable has the correct value to produce a zero eigenvalue in the above equation.

Interestingly, the number of additional dimensions due to the auxiliary qudits (slack variables) is proportional to N_r^{feas} , the number of feasible configurations of the corresponding constraint. Therefore, the more feasible configurations exist, the larger the dimension of the auxiliary qudit Hilbert space. The dimension of the full Hilbert space including the auxiliary slack qudits increases exponentially with the number of constraints, i.e., $\dim(\mathcal{H}_{\text{slack}}) = 2^N \prod_{r=1}^R N_r^{\text{feas}}$ and $\mathcal{H}_{\text{slack}} = \mathcal{H}_C \otimes \prod_{r=1}^R \mathbb{C}^{N_r^{\text{feas}}}$. However, given a feasible configuration $|\mathbf{x}\rangle$, only one state of the extended Hilbert space $|\mathbf{x}, \mathbf{s}\rangle$ will represent a feasible total state (the one with eigenvalue $s_r = -P_r(\mathbf{x})$), rendering the majority of added quantum states unfeasible. Thus, it can be anticipated that for only lightly constrained problems (that is, with large N_r^{feas}), the effective optimization problem including the slack variables is more difficult due to the large number of added unfeasible solutions.

The final form for the constrained Hamiltonian is then

$$H_{\text{slack}} = H_C + \sum_{r=1}^R \lambda_r (\hat{P}_r + \hat{S}_r)^2. \quad (18)$$

The quadratic form of the penalty terms guarantees that it can be made to vanish for all feasible configurations.

Adding qudit slack variables to the system requires modifications to the form of the QAOA-mixer as described at the end of Sec. II. Explicitly, we use the following form:

$$H_M = \beta \left(\sum_{i=1}^N \sigma_x^i + \sum_{r=1}^R L_x^{s_r} \right) + \gamma \sum_{r=1}^R (L_z^s)^2, \quad (19)$$

where both, β and γ are left as variational parameters. Apart from this change in the mixing operator, the QAOA is performed as described in Sec. II, just with the cost Hamiltonian given by Eq. (18).

B. Direct implementation of penalty terms for inequality constraints

We propose another possibility for including inequality constraints by using a penalized Hamiltonian of the form

$$H_{\text{penal}} = H_C + \sum_{r=1}^R \lambda_r \hat{G}_r, \quad (20)$$

where R is the total number of constraints and $\lambda_r > 0$ are penalty factors for each constraint. We introduced the operators \hat{G}_r whose eigenvalues depend on the corresponding constraint function given in Eq. (12), namely

$$\hat{G}_r |\mathbf{x}\rangle = g(P_r(\mathbf{x})) |\mathbf{x}\rangle. \quad (21)$$

For the function $g(\cdot)$ to penalize only the unfeasible states, it needs to be zero for non-positive arguments. To facilitate a gradient towards the feasible subspace, we moreover desire it to be non-decreasing for positive arguments. These requirements can be achieved by the following choice:

$$g(y) = y^a \Theta(y), \quad (22)$$

where $\Theta(y)$ is the Heaviside step function and $a \geq 0$ is an exponent that can be chosen freely. These types of penalty functions are illustrated in Fig. 1(d). The closest analogy to the slack-variable approach discussed in the previous section is achieved by the quadratic form, $a = 2$, but we will see in our numerical analysis in Sec. IV that $a = 1$ produces superior results

Including these penalties, the unitary operator to generate the trial wave function [Eq. (7)] is updated to

$$U(\boldsymbol{\alpha}, \boldsymbol{\beta}) = \prod_{l=1}^P e^{i\alpha_l H_{\text{penal}}} e^{i\beta_l H_M} \quad \text{with} \quad (23)$$

$$e^{i\alpha_l H_{\text{penal}}} = e^{i\alpha_l (H_C + \sum_{r=1}^R \lambda_r \hat{G}_r)}. \quad (24)$$

The rotation generated by the penalizing Hamiltonian puts phases $\sim \alpha_l \lambda_r$ on the unfeasible states, thus permitting the QAOA procedure to select them out.

Since the terms proportional to the constraints are diagonal in the computational basis, it is possible to find constructions either using Fourier analysis or ancilla registries [35, 36]. These methods are defined using only qubit systems and their efficiency is bound by the problem type and instance, and by the properties of the platform chosen for implementation.

In this work we propose an efficient implementation of diagonal unitaries of the form of Eqs. (23) and (24). In Appendix A, we describe the construction which is valid for constraint functions $P(\mathbf{x}) \leq 0$ which only depend on the Hamming weight (i.e., magnetization) $m = \sum_i x_i$ of the state $|\mathbf{x}\rangle$ of N qubits (generalization to summations of x_i and \bar{x}_i is straightforward). This construction uses one ancilla qudit along with $2(N_r - N_r^{\text{feas}})$ qudit SUM gates, where $N_r - N_r^{\text{feas}}$ is the number of unfeasible configurations. For the above constraint (13), this corresponds to the number of m values with $P(\sum_i x_i) > 0$, $g(m) > 0$.

In contrast to the slack-variable approach, the ancilla qudit does not enter the cost function, but serves only to imprint appropriate phases according to Eq. (24) onto the trial wavefunction. The bottleneck of this procedure is the ancilla dimensionality, as it needs to be at least equal to $N + 1$. However, since the ancilla qudit can be used for many constraints simultaneously, we can expect the proposed method to be advantageous in particular when many constraints are present simultaneously, with each involving only a restricted number of problem qubits and small to intermediate sets of possible values P_r .

C. Alternative approaches for inequality constraints from the literature

For completeness, we also mention other options that have been proposed in the literature. For example, one can start from a constrained state and perform the algorithm using only constraint-preserving evolution operators [37–39]. The drawback of this method is that usually such constraint-preserving operators are difficult to construct and need to be designed for each specific problem. Post-selection of feasible solutions [40] can also be used, but depending on the problem this may be very inefficient as finding feasible solutions at all can be difficult, especially for problems where several disconnected domains of feasible solutions exist. Inequalities can also be enforced by mid-circuit projection onto the feasible subspace through measurements of the constraint operators [41]. However, these projection operators are problem-specific and can be challenging to implement, while the necessary measurements contribute to both algorithmic and qubit overhead.

Another recent approach utilizes the augmented Lagrangian formulation of constrained optimization problems [42], which also introduces energy penalties into the optimization cost function. However, this approach is only effective for problems where the constraints are

active for the optimal solution, i.e., when the optimal solutions lie right at the boundary between feasible and unfeasible solutions such that the constraints become effective equality constraints.

IV. NUMERICAL BENCHMARKS

In this section, we show numerical results for QAOA performed in different scenarios where inequality constraints play a role. First, we analyze the ability of QAOA to obtain feasible solutions for a generic random spin model [43]. Then we show how to construct an initial constrained state for warm-starting the QAOA procedure. Finally, we test the performance on the industry-relevant problem of electric vehicle (EV) charging [44], which is subject to multiple constraints. For all of these problems, we compare the performance of the constraint-handling methods described in Secs. III A and III B.

We simulate the quantum part of the QAOA procedure using exact state vector simulations. To update the parameters defining the trial wavefunctions, we use the Powell classical optimizer from the `scipy` library [45]. For each problem instance, we perform $N_{\text{runs}} = 50$ separate runs, where for each run the variational parameters are initialized randomly in the interval $[0, 2\pi]$. For each finished QAOA run, we extract the classical solutions of the optimization problem by sampling $N_S = 64$ solutions (measurement shots) from the quantum state $|\psi(\alpha^*, \beta^*)\rangle$.

A. Metrics

We use various figures of merit to estimate the performance of the QAOA protocols under different constraint-handling techniques. As first metric, we consider the approximation ratio, which is defined as

$$R = \min_{\text{samples } s} \frac{E_s - E_0}{|E_0|}, \quad (25)$$

where E_s with $s = 1, \dots, N_S$ is the energy of a state sampled from the final state and E_0 is the feasible state with the lowest energy. This metric is relevant for studying the efficiency of QAOA in solving industrial optimization problems, since in such situations the user cares about the best energy of a single configuration that could be achieved, and not the average over the final state.

A second relevant figure of merit is the success rate, defined as

$$r = \frac{\sum_{i=1}^{N_{\text{runs}}} X_i}{N_{\text{runs}}}, \quad (26)$$

where N_{runs} is the total number of runs and $X_i = 1$ if the algorithm sampled at least one of the (possibly degenerate) optimal states in the N_S samples of the i -th run, and $X_i = 0$ otherwise.

A third figure of merit is the total weight of feasible solutions present in the final state,

$$W = \sum_{\mathbf{x} \in \text{feasible}} |c_{\mathbf{x}}(\boldsymbol{\alpha}^*, \boldsymbol{\beta}^*)|^2, \quad (27)$$

where the $c_{\mathbf{x}}(\boldsymbol{\alpha}^*, \boldsymbol{\beta}^*)$ are the amplitudes in the final QAOA state,

$$|\psi(\boldsymbol{\alpha}^*, \boldsymbol{\beta}^*)\rangle = \sum_{\mathbf{x}} c_{\mathbf{x}}(\boldsymbol{\alpha}^*, \boldsymbol{\beta}^*) |\mathbf{x}\rangle. \quad (28)$$

This metric serves as an indicator of the efficiency of the algorithm at sampling feasible solutions.

B. Random spin Hamiltonian

We start by studying the capabilities of QAOA in finding the ground state for a model of randomly interacting spin- $\frac{1}{2}$ in a random longitudinal field. We compare the qudit slack variables approach explained in III A to penalties discussed in III B. The cost Hamiltonian is

$$H_C = \sum_{i=1}^N h_i \sigma_i^z + \sum_{ij} J_{ij} \sigma_i^z \sigma_j^z, \quad (29)$$

with independent Gaussian-distributed parameters with zero mean and unit variance, i.e., $J_{ij}, h_i \sim \mathcal{N}(0, 1)$.

For this Hamiltonian, we consider a single constraint affecting all spins of the form

$$P(\boldsymbol{\sigma}_z) = \sum_{i=1}^N \sigma_i^z - m_0 \equiv S_{\text{tot}}^z - m_0 \leq 0, \quad (30)$$

which filters out all the states with total spin $S_{\text{tot}}^z = \sum_{i=1}^N \sigma_i^z$ less than a target $m_0 \in \{-\frac{N}{2}, \frac{N}{2} + 1, \dots, \frac{N}{2}\}$. For the penalties described in Section III B, we choose the exponent a to be equal to 0, 1, or 2, resulting in the penalty Hamiltonians

$$H_{a=0} = \lambda \Theta(S_{\text{tot}}^z - m_0), \quad (31a)$$

$$H_{a=1} = \lambda \Theta(S_{\text{tot}}^z - m_0) (S_{\text{tot}}^z - m_0), \quad (31b)$$

$$H_{a=2} = \lambda \Theta(S_{\text{tot}}^z - m_0) (S_{\text{tot}}^z - m_0)^2. \quad (31c)$$

When using the penalty term for the slack variables as described in Secs. III A, the complete cost Hamiltonian takes the form

$$H_{C,\text{slack}} = H_C + \lambda (S_{\text{tot}}^z - m_0 + \hat{S})^2, \quad (32)$$

where the slack variable operator \hat{S} acts on a qudit with dimension $d = \frac{N}{2} + 1 + m_0$.

We consider a system of $N = 9$ qubits, for which we study the metrics defined in Sec. IV A for a $p = 1$ layer

QAOA as a function of the value of the constrained magnetization m_0 . We generate 20 random realizations of the cost Hamiltonian and run $N_{\text{runs}} = 50$ simulations for each Hamiltonian. All the results shown are obtained for a penalty factor of $\lambda = 4$, but higher values for λ show similar results.

First, we investigate the efficiency of the different algorithms on the same problems as the dimension of the feasible subspace is increased. In Figs. 2 and 3, we compare the results obtained with the proposed method to the state-of-the-art approach using slack variables. We see that for all the metrics considered, the performance of the proposed approach is considerably better than that of the implementation with slack variables. For example, the success rate r for the penalties of Eqs. (31a)–(31c) is always significantly higher than for the slack-variable-based approach. Especially when m_0 approaches large values the proposed methods converge to $r \gtrsim 0.5$ while for slack variables it converges toward low values around $r \approx 0.1$. Similarly, the approximation ratio R for slack variables has only small fluctuations around 0.3 for values of m_0 greater than -2.5 , while for each instance of the approach based on direct penalization it quickly approaches 0 as m_0 increases and the system becomes less constrained.

Moreover, the performances of the flat, linear, and quadratic penalties can differ considerably. When considering r as figure of merit, the linear penalty shows the best behavior. Considering R for highly constrained problems ($m_0 \lesssim -1.5$) the best result is obtained with a flat penalty ($a = 0$). However, this effect is a direct result of the penalty terms in the Hamiltonian. Namely, for these problems the sampled low-energy states will also include unfeasible states, where the actual penalty term contributes to the energy, and consequently linear and quadratic terms will give larger energies in general.

Figure 3 shows the total weight of the feasible states as a function of the constraint target value m_0 , for the three forms of the penalty given in Eqs. (31a)–(31c) (left panel) as well as for the slack variable approach (right panel). The continuous lines show the total weight of the feasible states for a uniformly distributed quantum state as a baseline, which is simply given by the fraction of number of feasible states over all states (including qudit-slack variable states in case of slack-variable approaches), i.e., $\text{Base} = \dim(\mathcal{H}_{\text{feasible}}) / \dim(\mathcal{H}_{\text{tot}})$. For the proposed approach, the baseline increases monotonically from $1/2^N$ for $m_0 = -\frac{N}{2}$ toward 1 for the unconstrained problem at $m_0 = \frac{N}{2}$. In contrast, for the slack-variable approach it does not approach unity when increasing m_0 ; instead, it has a maximum around an intermediate value of $m_0 \approx 1.5$ and slightly decreases for larger m_0 . This behavior is due to the changing dimension of the slack variable with m_0 . On the one hand, the absolute number of feasible states for a given m_0 is the same as for the case without slack variables since only one out of all possible values for the slack variable represents a feasible solution. On the other hand, the dimension of the slack

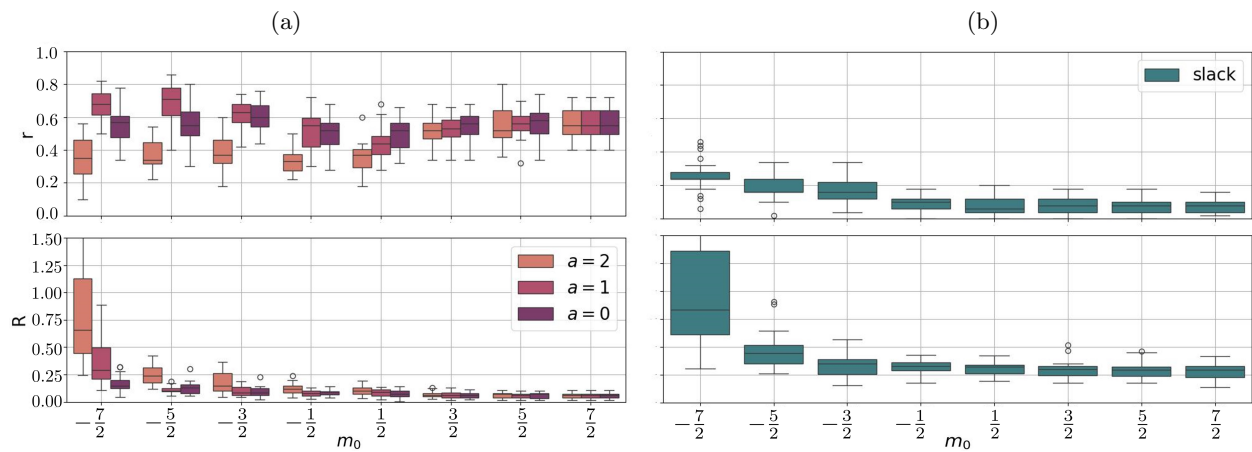


FIG. 2. Success rate r (top row) and approximation ratio R (bottom row) for constraint QAOA with a single layer ($p = 1$) and $N = 9$ qubits. The boxplots shows statistics for averages over 20 different instances of the random Hamiltonian of Eq. (29) and 50 runs per individual Hamiltonian. The results are shown as a function of the maximally allowed total spin, m_0 . (a) Results from the proposed approach directly implementing the penalty functions of Eqs. (31a)–(31c). The linear form ($a = 1$) consistently performs best when considering the success rate r , while the flat penalty shows best approximation ratio R . The results for different a become more similar as the value of m_0 increases, since the system becomes increasingly less constrained, reducing the impact of the different forms of penalties. (b) Results from runs using slack variables for handling the inequality constraints. The results clearly show the superiority of the direct penalty approaches of (a) over using slack variables as those achieve much higher success rates and lower approximation ratios.

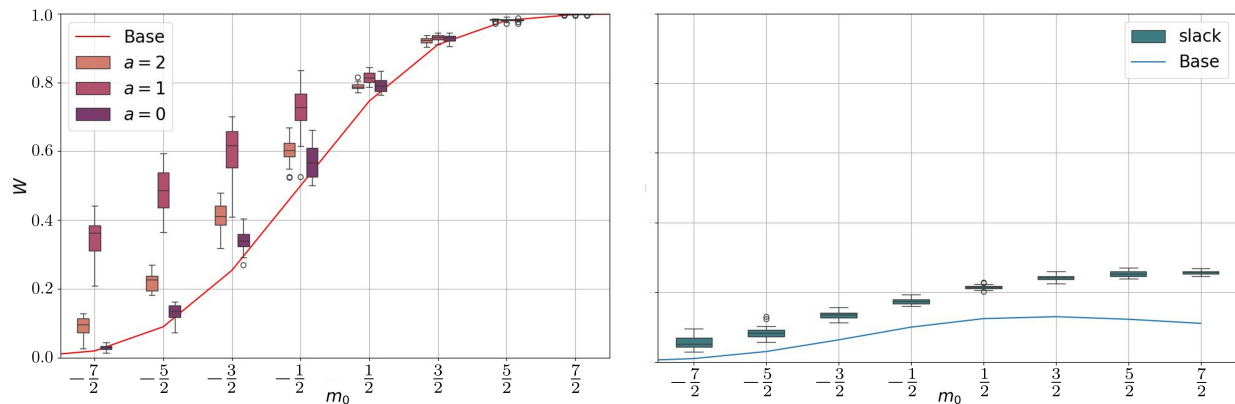


FIG. 3. Total weight W of all feasible states of single layer QAOA with constrained cost function defined in Eqs. (31a)–(31c) (left) and slack variables of Eq. (32) (right) for the same setup as Fig. 2. The solid lines show the baseline probability of finding a feasible state from an equal superposition of all basis states. The slack variable approach has consistently lower probability of sampling a feasible configuration from the final state, even if almost all qubit configurations are feasible for larger m_0 where it saturates around 25% while this probability reaches 100% for the proposed direct penalty method. This trend reflects what we see in Fig. 2 and serves as an indicator of the poor performance of slack variables for inequality-constrained optimization.

variable increases with increasing m_0 and thus in case of slack variables the baseline acquires an additional factor $\frac{1}{d} = 1/(m_0 + 1 + \frac{N}{2})$.

The results of Fig. 3 show that all the tested methods increase the probability of sampling a feasible state over the baseline. However, similarly to the trend of Fig. 2, the proposed direct penalty methods considerably outperform the slack variable approach. This effect is most pronounced for the linear penalty function and with increasing m_0 , i.e., for less constrained problems.

C. Constrained state preparation and sampling of feasible states

In certain scenarios, the goal of the algorithm may be to sample from a subset of states that fulfil the constraints, without any preference on the states within that subset. Examples include topological models and LGTs [46], spin ice [47], and the sampling of polymer melts [48, 49]. Another scenario is when trying to construct a superposition of many or all feasible states as it is required for the initialization of approaches utilizing

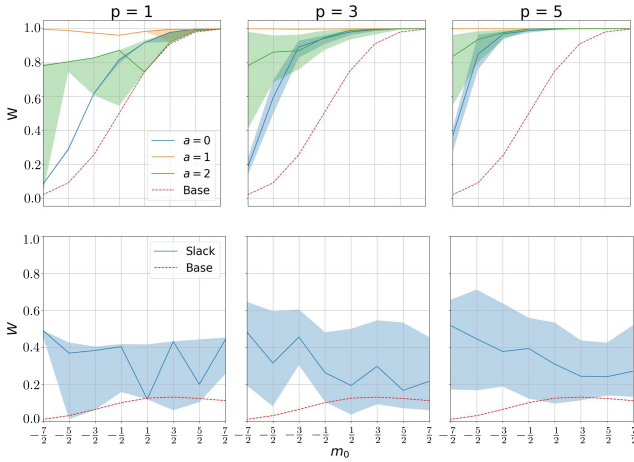


FIG. 4. Probability W of sampling a feasible state from the final state of a QAOA with constraint-only cost function, for the direct penalty approach (top row) and slack-variable based approach (bottom), for $p = 1, 3$, and 5 QAOA layers (left to right panels). The solid lines show median values for the different penalty types and the shaded areas indicate the 20%-80% quantiles of the 50 runs performed. The dashed red lines marked as ‘Base’ indicate the baseline probabilities from the equal superposition state of all solutions. The direct penalty functions outperform the slack-variable approach significantly. In particular, the penalty function with $a = 1$ gives close to 100% probability for all constraint values already for only $p = 1$ layer.

constraint preserving mixing operators [37–39].

Motivated by this, we consider a QAOA where the cost function is given only by the penalties encoding the constraint of the form of Eq. (30). The QAOA cost Hamiltonian is then of the form of Eqs. (31a)–(31c) for the proposed approach and of the form of Eq. (32) for the slack-variable approach. We run the QAOA for up to $p = 5$ layers, and we do $N_{\text{runs}} = 50$ for each setup (penalty type, number of layers, and constraint value m_0).

Figure 4 shows the total weight of feasible configurations in the final quantum state for numbers of layers $p = 1, 3$, and 5 . The linear penalty term considerably outperforms the slack-variable approach as well as the other penalty forms considered, reaching close to the maximum of $W = 1$ already after three layers for almost all values of the minimum magnetization m_0 . As in the previous example, all approaches improve as expected over the baseline, given by the weight of the feasible states on the initial state (dashed line). Again, for all chosen forms of the penalty function, the proposed direct penalty approach improves significantly more over the baseline than the slack-variable-based approach. As it would be expected, the direct approach also achieves overall better performances with increasing number of layers p . Interestingly such a trend is not observed for the slack-variable based approaches.

D. EV charging problem

To make contact with QAOA for solving combinatorics problems of industrial relevance and test the different approaches with multiple constraints, we evaluate the performance of the proposed approach for an electric vehicle (EV) charging problem. It is schematically represented in Fig. 1(a,b). The target of this problem is to find the charging schedule for a fleet of EVs, i.e., the charging power for each EV at each time step. This problem is naturally formulated in terms of qudit variables [21] as soon as more than two charging levels (charging or not charging) are considered. Importantly in our context, this problem naturally has many inequality constraints since each EV has minimum requirements for the total energy delivered to it while at each time step the total charging power must not exceed the fuse limits. It is thus a useful benchmark problem to study how the different approaches perform with the inclusion of multiple constraints.

The cost function of the considered EV charging problem is defined as

$$C(\mathbf{x}) = \sum_{t=1}^T c_t \sum_{n=1}^{N_{\text{EV}}} x_{n,t}, \quad (33)$$

where the variables $x_{n,t} \in \{x_{\min}, \dots, x_{\max}\}$ characterize the amount of energy charged (or discharged if $x_{\min} < 0$) to EV $n \in \{1, \dots, N_{\text{EV}}\}$ at time step $t \in \{1, \dots, T\}$. The (time-dependent) cost for a unit of electric energy is given by the coefficients c_t . This problem is naturally subject to many constraints. In particular, we consider the following two types:

$$E_n^{\text{required}} - \sum_{t=1}^T x_{n,t} \leq 0 \quad \forall n, \quad (34)$$

$$\sum_{n=1}^{N_{\text{EV}}} x_{n,t} - E^{\text{max}} \leq 0 \quad \forall t. \quad (35)$$

The first one, Eq. (34), reflects the requirement of each EV to obtain a minimal amount of electricity E_n^{required} after the charging is finished. The second constraint, Eq. (35), ensures that the maximal charging energy never exceeds the fuse limits. These are $N_{\text{EV}} + T$ linear constraints in total, where each couples only a specific subset of variables, but taken together they couple all variables with each other. This problem is illustrated in Fig. 1.

For demonstration purposes, we consider a rather simple problem instance where we only include two charging power levels, $x_{n,t} \in \{0, 1\}$ and two vehicles ($N_{\text{EV}} = 2$) for four time steps ($T = 4$). The constraints are specified by $E^{\text{max}} = 1$, and $E_0^{\text{required}} = E_1^{\text{required}} = 2$. With this setup, the classical combinations that satisfy the constraint are easy to define: each vehicle must be charged at least in two time steps, but the vehicles cannot be charged at the same time.

The quantum formulation is obtained by the usual replacement of the search variables with spin operators as shown in Eq. (3). The Hilbert space dimension for this simple example is $\dim(\mathcal{H}) = 2^{T \cdot N_{EV}} = 2^8 = 256$, out of which only 12 basis states are feasible. Due to the symmetry with respect to the EVs, the solutions are always doubly degenerate. To incorporate the constraints of Eqs. (34) and (35) using slack variables, we need a total of six auxiliary variables: two qudits for the constraints of Eq. (34) with dimension $d = 3$ and four qubits ($d = 2$) for those of Eq. (35). The Hilbert space dimension for the constrained problem is then $\dim \mathcal{H}_{\text{slack}} = 2^8 \cdot 3^2 \cdot 2^4 = 9216$, which is two orders of magnitude larger than the Hilbert space of the setup without slack variables.

We study the performance of QAOA as a function of the number of layers and for different random realizations of the Hamiltonian of Eq. (33), where the prices are chosen in each instance from a uniform distribution $c_t \sim \mathcal{U}(0, 1)$. We run $N_{\text{runs}} = 50$ runs for each problem instance. For the approach using direct penalties, we consider $p = 1, \dots, 5$ layers, while we did only run simulations for up to $p = 3$ layers for the slack-variable approach due to its vastly larger Hilbert-space dimension and the consequently significantly longer runtimes.

The results, summarized in Fig. 5, enhances the understanding of the previous benchmarks. The approach based on direct penalty Hamiltonians achieves success rates on the order of 30% already for $p = 1$, a value that increases up to 60%-90% for $p = 5$ layers. The approximation ratio also rapidly approaches zero with increasing p , especially for the best-performing case of $a = 1$.

In stark contrast, the results of the slack variable approach essentially indicate a failure of the method. Although the success rate does increase slightly for a larger number of layers, the overall scale is only around 10^{-3} . Similarly, the approximation ratio is an order of magnitude worse than for the direct penalty approach and essentially indicates that the algorithms never come close to finding the true ground-state energy region.

The reason for this failure is found in the vast increase in Hilbert-space dimension needed to encode all the different constraints. For each slack variable, only one of all possible configurations represents a feasible state, which leads to the majority of added states being unfeasible. In the above example where there are typically only two feasible configurations for the charging variables $x_{n,t}$, this leads to a reduction of the fraction of feasible solutions from $2/2^8 \approx 4 \cdot 10^{-3}$ without slack variables to $2/(2^8 \cdot 3^2 \cdot 2^4) \approx 5 \cdot 10^{-5}$ with slack variables. This large increase in search space due to the slack variables makes the corresponding search problem for the QAOA much more difficult.

V. CONCLUSION AND OUTLOOK

We have presented two approaches of using qudits to include energy penalties for an inequality-constrained QAOA routine: one by directly implementing energy penalties in a diagonal way and another by enlarging the system with ancilla qudits and introducing quadratic slack-variable-based penalty terms. We have benchmarked both approaches on three different problems, finding a significant difference in their performance. Specifically, including constraints directly without relying on additional qudits in the energy function vastly outperforms the slack-variable-based methods. Moreover, we find that a linear energy penalty outperforms the constant and quadratic penalty term.

Even if including the constraints through slack variables can lead to some decent results for a single constraint, the performance of this approach drops drastically when including multiple constraints. This is the typical case for a large class of combinatorial problems suited for QAOA (e.g., resource allocation problems [11]). Including many slack variables in the problem would be unfeasible for NISQ architectures. There, it leads to a drastic increase in required quantum resources that is hard to meet and in turn amplifies the noise in the circuit execution. In a fault-tolerant scheme where pure resources and noise are expected to not be the dominating limiting factors, it still considerably increases the complexity of the circuit, which is known to be a possible cause for the barren plateaus phenomenon [50]. Additionally, as shown in this work, the problem of finding low-energy states, i.e., the optimization problem to determine the parameters of the parameterized quantum circuit, is much more difficult to solve due to the vastly increased search space.

In the future, an interesting direction will be to combine the use of qudits for constraint handling and representation of the cost-function register, in order to maximize the use of available qudit levels in a given machine. Moreover, while qudit encodings of cost functions have been proposed, the potential performance advantages in variational quantum algorithms with respect to the usual qubit formulations need further thorough analysis, in particular also in view of the additional engineering overhead required. Our results may also stimulate cross-fertilization with other fields of quantum technologies. For example, including constraints in quantum algorithm is of fundamental relevance also for the task of quantum simulation of lattice gauge theories (LGTs) [51, 52], as these theories are characterized by an extensive set of physical constraints that needs to be preserved (e.g., Gauss' law in quantum electrodynamics) [53–55].

Further along the road, the proposed approach of including the energy penalties directly by using only a very small number of ancilla qudits, and thus avoiding the incorporation of slack variables into the energy functions, may be an enabling step for approaching realistic industry-scale and fundamental science problems with

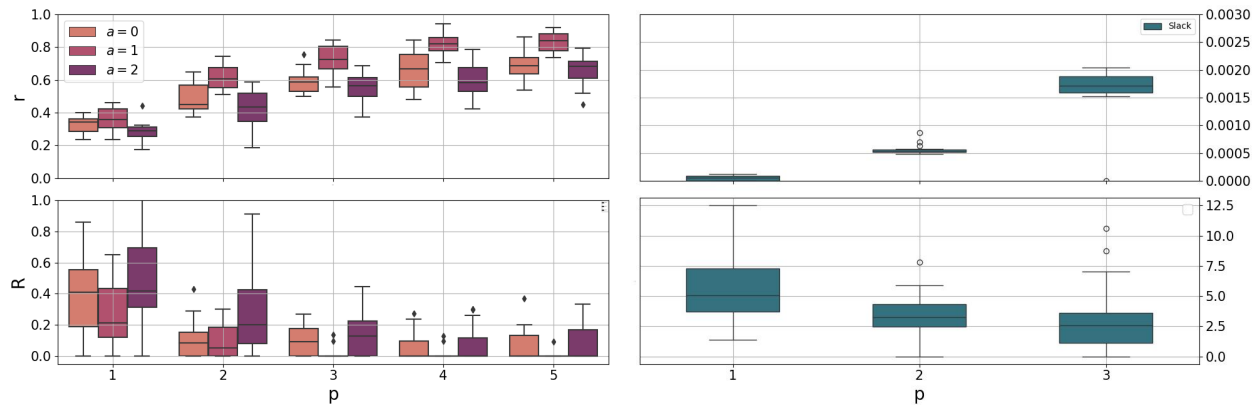


FIG. 5. Results of the EV charging problem of Eqs. (33) – (35) for $N_{\text{EV}} = 2$, $T = 4$, $E^{\text{max}} = 1$, and $E_n^{\text{required}} = 2$, for penalties encoded directly (left) and with slack variables (right) as function of the number of QAOA layers p . The approach based on direct penalty terms vastly outperforms the one based on slack-variables (note the different scale of the y axes). In line with the previous findings, the case with linear penalty $a = 1$ performs best among the direct penalty approaches. In particular, for $p \geq 3$ the median as well as the 20-th and the 80-th quantiles of the distribution of the approximation ratio R all vanish, indicating that an optimal solution is always found for $a = 1$.

large numbers of inequality constraints.

VI. ACKNOWLEDGEMENTS

We acknowledge fruitful discussions with Gopal Chandra Santra, Linus Ekstrøm, and Mikel Garcia de Andoin. A.B. acknowledges funding from the Honda Research Institute Europe. S.S. and P.H. acknowledge funding by the European Union under Horizon Europe Programme, Grant Agreement 101080086 — NeQST. This project has received funding from the Italian Ministry of University and Research (MUR) through the FARE grant for the project DAVNE (Grant R20PEX7Y3A), was supported by the Provincia Autonoma di Trento, and Q@TN, the joint lab between University of Trento, FBK—Fondazione Bruno Kessler,

INFN—National Institute for Nuclear Physics, and CNR—National Research Council. Project funded under the National Recovery and Resilience Plan (NRRP), Mission 4 Component 2 Investment 1.4 - Call for tender No. 1031 of 17/06/2022 of Italian Ministry for University and Research funded by the European Union – NextGenerationEU (proj. nr. CN_00000013). Project DYNAMITE QUANTERA2_00056 funded by the Ministry of University and Research through the ERANET COFUND QuantERA II – 2021 call and co-funded by the European Union (H2020, GA No 101017733). Views and opinions expressed are however those of the author(s) only and do not necessarily reflect those of the European Commission, the European Union or of the Ministry of University and Research. Neither the European Union nor the granting authority can be held responsible for them.

-
- [1] A. Abbas, A. Ambainis, B. Augustino, A. Bärtzchi, H. Buhrman, C. Coffrin, G. Cortiana, V. Dunjko, D. J. Egger, B. G. Elmegreen, N. Franco, F. Fratini, B. Fuller, J. Gacon, C. Gonciulea, S. Gribling, S. Gupta, S. Hadfield, R. Heese, G. Kircher, T. Kleinert, T. Koch, G. Korpas, S. Lenk, J. Marecek, V. Markov, G. Mazzola, S. Mensa, N. Mohseni, G. Nannicini, C. O’Meara, E. P. Tapia, S. Pokutta, M. Proissl, P. Rebentrost, E. Sahin, B. C. B. Symons, S. Tornow, V. Valls, S. Woerner, M. L. Wolf-Bauwens, J. Yard, S. Yarkoni, D. Zechiel, S. Zhuk, and C. Zoufal, arXiv:2312.02279 [10.48550/arXiv.2312.02279](https://arxiv.org/abs/2312.02279) (2023).
- [2] B. C. B. Symons, D. Galvin, E. Sahin, V. Alexandrov, and S. Mensa, arXiv:2305.07323 [10.48550/arXiv.2305.07323](https://arxiv.org/abs/2305.07323) (2023).
- [3] P. Hauke, H. G. Katzgraber, W. Lechner, H. Nishimori, and W. D. Oliver, *Reports on Progress in Physics* **83**, 054401 (2020).
- [4] S. Yarkoni, E. Raponi, T. Bäck, and S. Schmitt, *Reports on Progress in Physics* **85**, 104001 (2022).
- [5] K. Bharti, A. Cervera-Liarta, T. H. Kyaw, T. Haug, S. Alperin-Lea, A. Anand, M. Degroote, H. Heimonen, J. S. Kottmann, T. Menke, W.-K. Mok, S. Sim, L.-C. Kwek, and A. Aspuru-Guzik, *Rev. Mod. Phys.* **94**, 015004 (2022).
- [6] M. Cerezo, A. Arrasmith, R. Babbush, S. C. Benjamin, S. Endo, K. Fujii, J. R. McClean, K. Mitarai, X. Yuan, L. Cincio, *et al.*, *Nature Reviews Physics* **3**, 625 (2021).
- [7] J. Tilly, H. Chen, S. Cao, D. Picozzi, K. Setia, Y. Li, E. Grant, L. Wossnig, I. Rungger, G. H. Booth, and J. Tennyson, *Physics Reports* **986**, 1 (2022), the Variational Quantum Eigensolver: a review of methods and best practices.
- [8] D. A. Fedorov, B. Peng, N. Govind, and Y. Alexeev, *Materials Theory* **6**, 2 (2022).

- [9] E. Farhi, J. Goldstone, and S. Gutmann, arXiv:1411.4028 [10.48550/arXiv.1411.4028](https://arxiv.org/abs/10.48550/arXiv.1411.4028) (2014).
- [10] K. Blekos, D. Brand, A. Ceschini, C.-H. Chou, R.-H. Li, K. Pandya, and A. Summer, *Physics Reports* **1068**, 1 (2024), a review on Quantum Approximate Optimization Algorithm and its variants.
- [11] S. Limmer, J. Varga, and G. R. Raidl, *Energies* **16**, [10.3390/en16124576](https://arxiv.org/abs/10.3390/en16124576) (2023).
- [12] M. S. Blok, V. V. Ramasesh, T. Schuster, K. O'Brien, J. M. Kreikebaum, D. Dahlen, A. Morvan, B. Yoshida, N. Y. Yao, and I. Siddiqi, *Phys. Rev. X* **11**, 021010 (2021).
- [13] M. Ringbauer, M. Meth, L. Postler, R. Stricker, R. Blatt, P. Schindler, and T. Monz, *Nature Physics* **18**, 1053 (2022).
- [14] V. Kasper, D. González-Cuadra, A. Hegde, A. Xia, A. Dauphin, F. Huber, E. Tiemann, M. Lewenstein, F. Jendrzejewski, and P. Hauke, *Quantum Science and Technology* **7**, 015008 (2022).
- [15] Y. Chi, J. Huang, Z. Zhang, J. Mao, Z. Zhou, X. Chen, C. Zhai, J. Bao, T. Dai, H. Yuan, *et al.*, *Nature communications* **13**, 1166 (2022).
- [16] D. González-Cuadra, T. V. Zache, J. Carrasco, B. Kraus, and P. Zoller, *Physical Review Letters* **129**, 160501 (2022).
- [17] P. Hrmo, B. Wilhelm, L. Gerster, M. W. van Mourik, M. Huber, R. Blatt, P. Schindler, T. Monz, and M. Ringbauer, *Nature Communications* **14**, 2242 (2023).
- [18] X. Gao, P. Appel, N. Friis, M. Ringbauer, and M. Huber, *Quantum* **7**, 1141 (2023).
- [19] L. E. Fischer, A. Chiesa, F. Tacchino, D. J. Egger, S. Carretta, and I. Tavernelli, *PRX Quantum* **4**, 030327 (2023).
- [20] S. Bravyi, A. Kliesch, R. Koenig, and E. Tang, *Quantum* **6**, 678 (2022).
- [21] Y. Deller, S. Schmitt, M. Lewenstein, S. Lenk, M. Federer, F. Jendrzejewski, P. Hauke, and V. Kasper, *Phys. Rev. A* **107**, 062410 (2023).
- [22] G. Bottrill, M. Pandey, and O. Di Matteo, in *2023 IEEE International Conference on Quantum Computing and Engineering (QCE)*, Vol. 01 (2023) pp. 177–183.
- [23] M. Karácsony, L. Oroszlány, and Z. Zimborás, arXiv preprint arXiv:2302.07357 (2023).
- [24] E. Farhi and A. W. Harrow, arXiv:1602.07674 [10.48550/arXiv.1602.07674](https://arxiv.org/abs/10.48550/arXiv.1602.07674) (2019).
- [25] G. Kochenberger, J.-K. Hao, F. Glover, M. Lewis, Z. Lü, H. Wang, and Y. Wang, *Journal of combinatorial optimization* **28**, 58 (2014).
- [26] A. Lucas, *Frontiers in Physics* **2**, [10.3389/fphy.2014.00005](https://arxiv.org/abs/10.3389/fphy.2014.00005) (2014).
- [27] P. Giorda, P. Zanardi, and S. Lloyd, *Physical Review A* **68**, 062320 (2003).
- [28] N. L. Wach, M. S. Rudolph, F. Jendrzejewski, and S. Schmitt, *Quantum Mach. Intell.* **5**, 36 (2023).
- [29] arXiv:2308.16230 (2023).
- [30] D. H. Useche, A. Giraldo-Carvajal, H. M. Zuluaga-Bucheli, J. A. Jaramillo-Villegas, and F. A. González, *Quantum Inf Process* **21**, 12 (2022).
- [31] M. G. De Andoin, A. Bottarelli, S. Schmitt, I. Oregi, P. Hauke, and M. Sanz, in *2023 IEEE 26th International Conference on Intelligent Transportation Systems (ITSC)* (2023) pp. 5318–5323.
- [32] V. Vargas-Calderón, N. Parra-A., H. Vinck-Posada, and F. A. González, *Journal of the Physical Society of Japan* **90**, 114002 (2021).
- [33] K. Kuroiwa and Y. O. Nakagawa, *Phys. Rev. Res.* **3**, 013197 (2021).
- [34] J. Nocedal and S. J. Wright, *Numerical Optimization*, Springer Series in Operations Research and Financial Engineering (Springer, 2006).
- [35] J. Welch, D. Greenbaum, S. Mostame, and A. Aspuru-Guzik, *New Journal of Physics* **16**, 033040 (2014).
- [36] S. Hadfield, *ACM Transactions on Quantum Computing* **2**, 1 (2021).
- [37] F. G. Fuchs, K. O. Lye, H. Møll Nilsen, A. J. Stasik, and G. Sartor, *Algorithms* **15**, 202 (2022).
- [38] S. Hadfield, Z. Wang, B. O’Gorman, E. G. Rieffel, D. Venturelli, and R. Biswas, *Algorithms* **12**, 34 (2019).
- [39] A. Bärttschi and S. Eidenbenz, in *2020 IEEE International Conference on Quantum Computing and Engineering (QCE)* (2020) pp. 72–82.
- [40] P. Díez-Valle, J. Luis-Hita, S. Hernández-Santana, F. Martínez-García, Álvaro Díaz-Fernández, E. Andrés, J. J. García-Ripoll, E. Sánchez-Martínez, and D. Porras, *Quantum Science and Technology* **8**, 045009 (2023).
- [41] D. Herman, R. Shaydulin, Y. Sun, S. Chakrabarti, S. Hu, P. Minssen, A. Rattew, R. Yalovetzky, and M. Pistoia, *Communications Physics* **6**, 219 (2023).
- [42] H. N. Djidjev, *Advanced Quantum Technologies* **6**, 2300104 (2023).
- [43] N. Sauerwein, F. Orsi, P. Urich, S. Bandyopadhyay, F. Mattiotti, T. Cantat-Moltrecht, G. Pupillo, P. Hauke, and J.-P. Brantut, *Nature Physics* **19**, 1128 (2023).
- [44] O. Sassi and A. Oulamara, *International Journal of Production Research* **55**, 519 (2017).
- [45] P. Virtanen, R. Gommers, T. E. Oliphant, M. Haberland, T. Reddy, D. Cournapeau, E. Burovski, P. Peterson, W. Weckesser, J. Bright, S. J. van der Walt, M. Brett, J. Wilson, K. J. Millman, N. Mayorov, A. R. J. Nelson, E. Jones, R. Kern, E. Larson, C. J. Carey, Í. Polat, Y. Feng, E. W. Moore, J. VanderPlas, D. Laxalde, J. Perktold, R. Cimrman, I. Henriksen, E. A. Quintero, C. R. Harris, A. M. Archibald, A. H. Ribeiro, F. Pedregosa, P. van Mulbregt, and SciPy 1.0 Contributors, *Nature Methods* **17**, 261 (2020).
- [46] A. Y. Kitaev, *Annals of physics* **303**, 2 (2003).
- [47] M. Udagawa, L. Jaubert, *et al.*, *Spin Ice* (Springer, 2021).
- [48] C. Micheletti, P. Hauke, and P. Faccioli, *Physical Review Letters* **127**, 080501 (2021).
- [49] F. Slongo, P. Hauke, P. Faccioli, and C. Micheletti, *Science Advances* **9**, eadi0204 (2023).
- [50] M. Larocca, S. Thanasilp, S. Wang, K. Sharma, J. Biamonte, P. J. Coles, L. Cincio, J. R. McClean, Z. Holmes, and M. Cerezo, arXiv preprint arXiv:2405.00781 (2024).
- [51] M. C. Banuls, R. Blatt, J. Catani, A. Celi, J. I. Cirac, M. Dalmonte, L. Fallani, K. Jansen, M. Lewenstein, S. Montangero, *et al.*, *The European physical journal D* **74**, 1 (2020).
- [52] J. C. Halimeh, M. Aidelsburger, F. Grusdt, P. Hauke, and B. Yang, arXiv preprint arXiv:2310.12201 (2023).
- [53] J. C. Halimeh, H. Lang, J. Mildnerberger, Z. Jiang, and P. Hauke, *PRX Quantum* **2**, 040311 (2021).

- [54] J. C. Halimeh and P. Hauke, arXiv preprint arXiv:2204.13709 (2022).
 [55] A. Rajput, A. Roggero, and N. Wiebe, npj Quantum Information **9**, 41 (2023).

Appendix A: Penalties for Hamming weight constraints

This appendix shows how to implement unitaries of the Hamiltonians (31) using a qudit ancilla. There exist ways to exponentiate arbitrary boolean functions in quantum computers. In general, these require computing the Fourier transform of the function that needs to be exponentiated. In principle, this allows to implement diagonal unitaries of the form of Eq. (24), albeit with unfavorable, typically exponential, scaling in the number of gates (see, e.g., [35, 36]) or with a problem-dependent reduced gate count.

Here, we provide an alternative way to implement such a unitary using only one ancilla qudit and without the need to compute the Fourier transform. We assume a unitary U_g that is parametrized by a function $g(m)$ that only depends on the total Hamming weight (or magnetization)

$$m(\mathbf{x}) = \sum_{i=1}^N x_i \quad (\text{A1})$$

of the N -qubit basis state

$$|\mathbf{x}\rangle = |x_1, x_2, \dots, x_N\rangle \quad (x_i \in \{0, 1\}). \quad (\text{A2})$$

This is a common constraint that appears in many scheduling problems such as the EV charging problem.

For a N qubit state, the Hamming weight can take the $N + 1$ integer values $m \in \{0, 1, \dots, N\}$, and the function $g(m)$ can have any functional dependence on m . For our purposes of implementing penalty terms, we assume that it is non-negative for a given subset \mathcal{I} of all possible values for m ,

$$g(m) > 0 \text{ for } m \in \mathcal{I}. \quad (\text{A3})$$

For the other states, the function is taken to be zero to indicate feasible states, i.e., $g(m) = 0$ for $m \notin \mathcal{I}$. The number of infeasible values for m is denoted by $N_{\mathcal{I}} = |\mathcal{I}|$.

The construction to implement such a function is valid if the action of the unitary U_g can be implemented in a controlled way, where the control state is the ancilla qudit,

$$|y\rangle_a \text{ with } y \in \{0, 1, \dots, N\}. \quad (\text{A4})$$

The dimension of the ancilla qudit is determined by the number of qubits, $N + 1$.

The circuit implementing the proposed approach is depicted in Fig. 6. We start from a product state of the

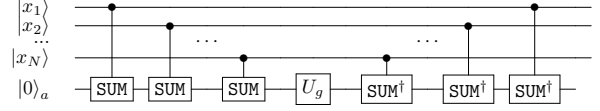


FIG. 6. Circuit showing how an arbitrary phase $g(m)$ as function of the magnetization $m(\mathbf{x}) = \sum_i x_i$ can be applied on the qubit register using one ancilla qudit $|y\rangle_a$.

problem qubits, which can be in an arbitrary state, and the ancilla qudit, which is initialized in $|0\rangle_a$, i.e.,

$$|\psi\rangle |0\rangle_a = \sum_{\mathbf{x}} c_{\mathbf{x}} |\mathbf{x}\rangle |0\rangle_a. \quad (\text{A5})$$

Then, we apply a SUM gate that adds the boolean value corresponding to one of the qubits onto the target ancilla. Repeating this operation for each qubit, we end up in a state where the ancilla qudit has the value $m = m(\mathbf{x}) = \sum_i x_i$,

$$\prod_i \text{SUM}_{i \rightarrow a} |\psi\rangle |0\rangle_a = \sum_{\mathbf{x}} c_{\mathbf{x}} |\mathbf{x}\rangle |m\rangle_a. \quad (\text{A6})$$

After that, we apply a simple phase shift to the ancilla qudit such that $U_g |m\rangle = e^{ig(m)} |m\rangle$. This operation takes the state to

$$\sum_{\substack{\mathbf{x} \\ m(\mathbf{x}) \notin \mathcal{I}}} c_{\mathbf{x}} |\mathbf{x}\rangle U_g |m\rangle_a + \sum_{\substack{\mathbf{x} \\ m(\mathbf{x}) \in \mathcal{I}}} c_{\mathbf{x}} |\mathbf{x}\rangle U_g |m\rangle_a \quad (\text{A7})$$

$$= \sum_{\substack{\mathbf{x} \\ m(\mathbf{x}) \notin \mathcal{I}}} c_{\mathbf{x}} |\mathbf{x}\rangle |m\rangle_a + \sum_{\substack{\mathbf{x} \\ m(\mathbf{x}) \in \mathcal{I}}} c_{\mathbf{x}} e^{ig(m)} |\mathbf{x}\rangle |m\rangle_a. \quad (\text{A8})$$

After undoing the SUM gates, the final state is

$$\left(\sum_{\substack{\mathbf{x} \\ m(\mathbf{x}) \notin \mathcal{I}}} c_{\mathbf{x}} |\mathbf{x}\rangle + \sum_{\substack{\mathbf{x} \\ m(\mathbf{x}) \in \mathcal{I}}} c_{\mathbf{x}} e^{ig(m)} |\mathbf{x}\rangle \right) |0\rangle_a, \quad (\text{A9})$$

which realizes the desired application of the unitary parameterized by a function $g(m)$ on the qubit quantum state $|\psi\rangle$. For the case of the constraints we consider, g has the form

$$g(m) = \Theta(m - m_0) (m - m_0)^a. \quad (\text{A10})$$

and the corresponding final state is

$$\left(\sum_{\substack{\mathbf{x} \\ m(\mathbf{x}) \notin \mathcal{I}}} c_{\mathbf{x}} |\mathbf{x}\rangle + \sum_{\substack{\mathbf{x} \\ m(\mathbf{x}) \in \mathcal{I}}} c_{\mathbf{x}} e^{i(m(\mathbf{x}) - m_0)^a} |\mathbf{x}\rangle \right) |0\rangle_a \quad (\text{A11})$$

which adds a phase to those states with $m \in \mathcal{I} = \{m_0 + 1, m_0 + 2, \dots, N\}$.

The entire procedure for arbitrary $g(m)$ requires only $2N$ qudit controlled SUM gates and a single qudit phase

shift unitary. A requirement for it to work is the availability of qudits with at least N levels, where N is the number of qubits involved in the constraint. This procedure becomes thus particularly favourable when many constraints acting on restricted sets of qubits are present.

The above procedure can also be generalized to penal-

ties which depend on functions of m^* , where

$$m^*(\mathbf{x}) = \sum_{i \in N} x_i + \sum_{i \in \bar{N}} \bar{x}_i. \quad (\text{A12})$$

N and \bar{N} are two distinct subsets of the system qubits. One needs only to include a π -rotation (σ_x) for each qubit belonging to set \bar{N} before (after) the SUM-gate (SUM † -gate).